engineering proceedings

MDPI

Proceeding Paper

Fault Diagnosis of the Vehicle Lateral System Using Bayesian Networks and EKF with Real-Time ROS Applications †

Tolga Bodrumlu *, Murat Gozum, Batıkan Kavak and Eyüp Ateş

AVL Türkiye Research and Engineering, Istanbul, 93049, Türkiye; murat.gozum@avl.com (M.G.); batikan.kavak@avl.com (B.K.); eyup.ates@avl.com (E.A.)

* Correspondence: tolga.bodrumlu@avl.com

† Presented at The 11th International Electronic Conference on Sensors and Applications (ECSA-11), 26–28 November 2024; Available online: https://sciforum.net/event/ecsa-11.

Abstract: In various engineering applications, model-based fault diagnosis techniques are used as analytical models to reduce the computational cost associated with existing empirical models. Due to their robustness, Bayesian Network-based methods have become particularly popular among other model-based techniques. This article introduces a model-based fault diagnosis approach that combines Bayesian Network and Extended Kalman Filter to detect faults in a vehicle's lateral dynamic system. Residual values of yaw rate, wheel slip rate, and steering angle are calculated by comparing sensor data with data obtained from analytical models. The vehicle's speed is estimated with the Extended Kalman Filter (EKF) using GPS and accelerometer data, and potential errors in the wheel speed sensors are detected. In case of an incorrect wheel speed measurement, detection occurs, and the speed value obtained from sensor fusion is transferred to the dynamic model. The proposed method is first modeled and tested in the Matlab/Simulink environment. Subsequently, the C++ implementation in ROS (Robot Operating System) which also contains the communication structure between the vehicle and algorithm is completed. Furthermore, in order to display the errors visually in real-time tests, a Human-Machine Interface (HMI) is developed. Results of the real-time tests indicate clearly that the designed algorithm can detect errors with high accuracy.

Keywords: fault diagnosis; extended Kalman filter; Bayesian network; ROS

Citation: Bodrumlu, T.; Gozum, M.; Kavak, B.; Ateş, E. Fault Diagnosis of the Vehicle Lateral System Using Bayesian Networks and EKF with Real-Time ROS Applications. *Eng. Proc.* **2024**, *6*, x. https://doi.org/10.3390/xxxxx

Academic Editor(s): Name

Published: 26 November 2024

Copyright: © 2024 by the authors. Submitted for possible open access publication under the terms and conditions of the Creative Commons Attribution (CC BY) license (https://creativecommons.org/licenses/by/4.0/).

1. Introduction

As a consequence of innovative fault detection and diagnosis techniques the safety and reliability of technical processes have advanced [1–4]. Recently, model-based fault detection techniques have become a popular choice because of their analytical redundancy [5]. In these techniques, the quantity calculated from the analytical models is compared with the measured quantity by using analytical redundancy [6]. Not only does model-based fault detection provide reliable results thanks to its analytical redundancy, it is also advantageous in terms of cost since it does not cause any additional cost or weight burdens. That being said, the importance of model choice and how updates are made should be kept in mind. As a result, these methods play an important role in increasing the security and reliability of technical processes. Fault trees are another commonly used method for diagnosing faults. In this method, the user is asked a series of questions containing possible fault symptoms and the goal is to try and determine the cause of the fault according to the user's answers to these questions [7,8]. Although fault trees are a practical and user-friendly approach, they have some significant drawbacks. For example, cases where judgment about a particular failure cause is uncertain are not addressed by the model. Additionally, the fixed nature of the tree prevents the integration of expertise or previous knowledge into the diagnostic process and can make it difficult to detect faults with multiple symptoms [9]. Signal-based fault detection systems are another alternative

and effective method used to detect faults in complex systems [10]. This method detects faults by analyzing the measured output signals of the system. Faults in the system are usually associated with and detected through changes in the properties of the measured signals. Signal-based fault detection does not rely on mathematical models to realize fault diagnosis, thus the difficulty of dealing with the complexity and uncertainty of system modeling is avoided. In [12], the authors used model-based and signal-based approaches to perform fault diagnosis on an induction motor and concluded that although the model-based approach is more difficult to implement due to the complexity of the models used it performs better than the signal-based approach.

In this paper, a model-based fault detection algorithm is developed for the lateral dynamics of an autonomous vehicle with non-constant longitudinal velocity. The developed fault detection algorithm includes both Bayesian Network and Extended Kalman Filter (EKF). Since the dynamic model used in the algorithm works with the integration of vehicle speed data, even a single incorrect measurement of speed data can disrupt the dynamic structure of the entire system. This problem is mitigated by using the EKF structure. Six residual values are calculated in the fault detection algorithm. The first three residual values are calculated by comparing the yaw speed measured by the gyroscope with the yaw speed values obtained from the front wheels, rear wheels, and the dynamic bicycle model, respectively. Two additional residual values are calculated by comparing the slip rate obtained from sensor measurements of the right and left wheels with the slip rate obtained from the tire model. The final residual value is calculated by taking the difference between the value obtained from the steering angle sensor and the steering angle calculated from the steering angle model. If there is an incorrect wheel speed measurement, this is detected, and the speed value obtained from sensor fusion is used in the dynamic model instead. Threshold values of all calculated residuals are determined using datasets collected from an autonomous testing vehicle. Depending on whether the residuals exceed the threshold value, the coefficients of the Bayesian Network are dynamically updated to decide which sensor or actuator is faulty. The results show us that robust and accurate fault detection is achieved using Bayesian Network and EKF. Visualization of the system and occurring faults are achieved in a user-friendly manner by incorporating an HMI interface to the system.

2. Fault Diagnosis Structure

2.1. Sensors Used to Obtain Residuals

In this paper, residual values for yaw rate, slip rate and steering angle are obtained. In Table 1, the symbols of both the values included in the analytical models used and the sensors from which the resulting measurements were made are given.

Table 1. Symbols and explanations of parameters measured with the sensors.

Symbol	Explanation
V_{FL}	Front Left Wheel Speed
V_{FR}	Front Right Wheel Speed
V_{RL}	Rear Left Wheel Speed
V_{RR}	Rear Right Wheel Speed
δ	Steering Wheel Angle
$\dot{\psi}$	Yaw Rate

2.2. Residual Models

In this study, six residual values that enable fault diagnosis are obtained from six different models. Details of these models are given in [13]. Three of these models are used to calculate the yaw rate. Two models are used to calculate wheel slip rate, and the last remaining model is used to calculate the steering angle. The linear bicycle model is first

used to calculate the yaw rate. The state-space equation of the linear bicycle model is shown in Equation (1) [14]:

$$\begin{bmatrix}\dot{y}\\ \ddot{y}\\ \dot{\psi}\\ \ddot{\psi}\end{bmatrix}=\begin{bmatrix}0 & 1 & 0 & 0\\ 0 & -\frac{2C_{af}+2C_{ar}}{mV_x} & 0 & -V_x-\frac{2C_{af}l_f-2C_{ar}l_r}{mV_x}\\ 0 & 0 & 0 & 1\\ 0 & -\frac{2l_fC_{af}-2l_rC_{ar}}{I_zV_x} & 0 & -\frac{2l_f^2C_{af}+2l_r^2C_{ar}}{I_zV_x}\end{bmatrix}\begin{bmatrix}y\\ \dot{y}\\ \dot{\psi}\\ \dot{\psi}\end{bmatrix}+\begin{bmatrix}0\\ \frac{2C_{af}}{m}\\ 0\\ \frac{2l_fC_{af}}{I_z}\end{bmatrix}\delta \quad (1)$$

Apart from the bicycle model, the yaw rate based on the front and rear wheel speed models is also calculated. These models are given in Equations (2) and (3) and shown below [15]:

$$\dot{\psi}=(V_{FR}-V_{FL})/b_f \quad (2)$$

$$\dot{\psi}=(V_{RR}-V_{RL})/b_r \quad (3)$$

In calculating the wheel slip rate, the relationship depending on whether the front or rear wheel is driven is used [14]. This relationship is shown in Equation (4):

$$S=\frac{\omega_{undriven}-\omega_{driven}}{\omega_{undriven}} \quad (4)$$

Assuming linear conditions, the wheel slip rate can also be calculated using Equation (5) [15]:

$$F_x=\frac{1}{2}ma_x=C_xS \quad (5)$$

Finally, Equation (6) is used to calculate the steering angle:

$$\hat{\delta}=\frac{l\cdot i_{st}}{V_x}\dot{\psi} \quad (6)$$

2.3. Fault Diagnosis Plan

The three residual values related to the yaw rate are calculated by subtracting the yaw rate values obtained using the analytical models from the yaw rate measurements obtained from the sensors:

$$\begin{aligned}R_1&=\hat{\dot{\psi}}_{model_1}-\dot{\psi}_{sensor}\\ R_2&=\hat{\dot{\psi}}_{model_2}-\dot{\psi}_{sensor}\\ R_3&=\hat{\dot{\psi}}_{model_3}-\dot{\psi}_{sensor}\end{aligned} \quad (7)$$

Here, $model_1$, $model_2$, and $model_3$ represent the bicycle, front wheel, and rear wheel speed models, respectively. When the slip ratios obtained from the left and right wheel speeds (Equation (4)) are subtracted from the slip ratios obtained by the force relationship of the driven wheels on both sides of the vehicle (Equation (5)), two more residuals can be calculated:

$$\begin{aligned}R_4&=S_{force\ relation}-S_{right\ wheel\ speeds}\\ R_5&=S_{force\ relation}-S_{left\ wheel\ speeds}\end{aligned} \quad (8)$$

The final residual value is obtained by subtracting the steering angle sensor value from the steering angle value obtained through the analytical model shown in Equation (6):

$$R_6=\hat{\delta}_{model}-\delta_{sensor} \quad (9)$$

A total of 10 faults have been determined that these residuals can be used together with the Bayesian network to achieve fault diagnosis. Six of these faults are sensor faults and 4 of them are physical faults. These are presented in Table 2 below:

Table 2. Faults Table.

Fault	Explanation
F_1	Front Right Tire Physical Fault
F_2	Front Left Tire Physical Fault
F_3	Rear Right Tire Physical Fault
F_4	Rear Left Tire Physical Fault
F_5	Front Right Tire Sensor Fault
F_6	Front Left Tire Sensor Fault
F_7	Rear Right Tire Sensor Fault
F_8	Rear Left Tire Sensor Fault
F_9	Yaw Rate Sensor Fault
F_{10}	Road Wheel Angle Sensor Fault

The directed graph that depicts the relation between the faults and residuals is presented in Figure 1 below.

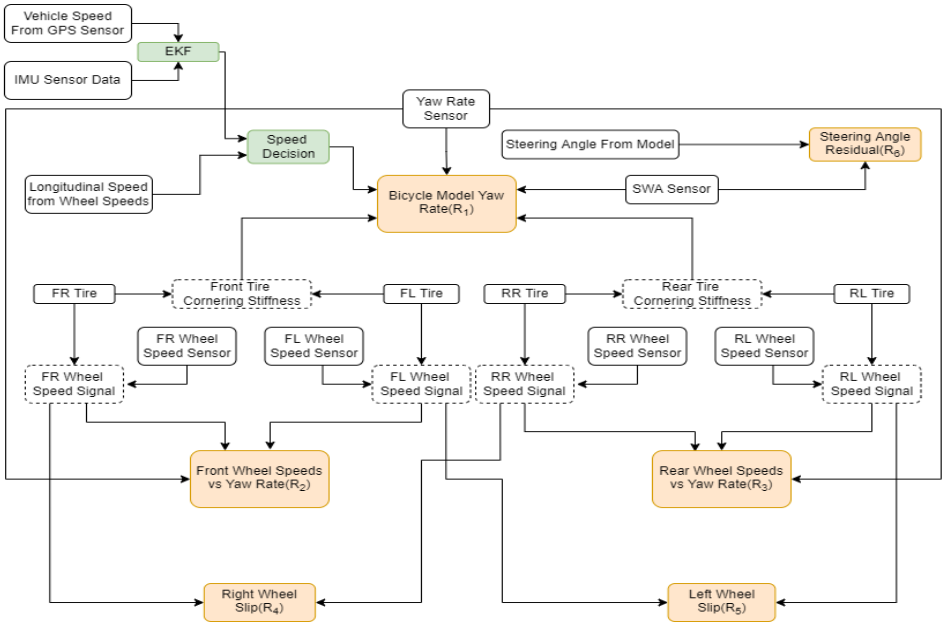

Figure 1. Directed graph of the fault diagnosis structure.

2.4. Dynamic Bayesian Network

In this study, failure probabilities are calculated using a Bayesian network. Depending on the structure used, when any residual value is active, the probabilities of faults related to it are dynamically updated. As shown in Figure 1, there are faults that affect each residual value. The logic and detailed explanation of the created dynamic Bayesian network are explained in a previous publication of the authors [11]. Table 3 shows which faults are active for certain residual values.

Table 3. The faults and the corresponding residuals.

R_1	R_2	R_3	R_4	R_5	R_6	Faults
1	0	0	0	0	1	F_{10}
1	0	1	0	1	0	F_4
1	1	0	1	0	0	F_1
1	1	0	0	1	0	F_2
1	0	1	1	0	0	F_3

1	0	1	0	1	1	F_8, F_{10}
1	1	0	0	1	1	F_6, F_{10}
1	1	0	1	0	1	F_5, F_{10}
1	0	1	1	0	1	F_7, F_{10}
1	1	1	0	0	1	F_9, F_{10}

2.5. Extended Kalman Filter

One of the inputs of the bicycle model is the vehicle speed calculated from the speed data from the wheel sensors. Therefore, a faulty speed measurement from any wheel will cause the bicycle model to miscalculate the yaw rate. In this case, the fault diagnosis algorithm will determine that the fault is in the yaw rate, when in reality it is mainly caused by the speed data. In order to solve this problem, the fault detection algorithm obtains the speed data of the vehicle by combining the speed data received from the GPS sensor and the accelerometer data received from the IMU sensor with the help of Extended Kalman Filter (EKF). The general structure of the EKF is shown in Figure 2. At this point, this combined speed data should be used instead of the speed value from the wheel speed sensors to prevent incorrect calculation of the yaw rate obtained by the bicycle model.

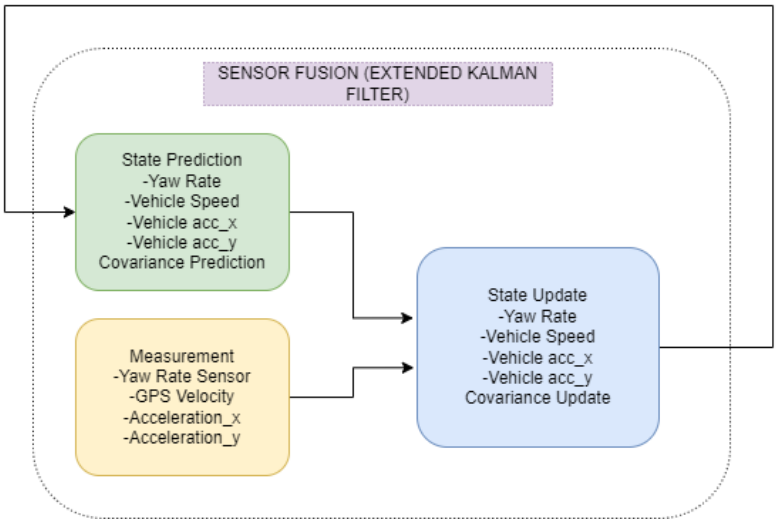

Figure 2. EKF structure.

2.6. ROS Structure

The Bayesian Network structure explained in Section 2.4 has been implemented and tested in an autonomous test vehicle both in a simulation and real-world. While doing this, the Melodic version of ROS has been used on Ubuntu v18.04.

A ROS package containing the Fault Detection node has been created to obtain the probabilistic output of each fault. Accordingly, functions have been implemented to calculate the residual values at the end of each cycle of the node. The sensor readings required to be used in the calculation of these residual values are obtained by subscribing to the topic of the associated sensor. Following the calculation of the residual values, these values become the input of another function whose duty is to create the Bayesian Network and then calculate the failure probabilities. Finally, these probabilities are published to the Bayes topic by creating a message type that makes it possible to visualize each of the faults. The applied ROS structure is visually summarized in Figure 3. In the next section, the simulation system is explained in more detail.

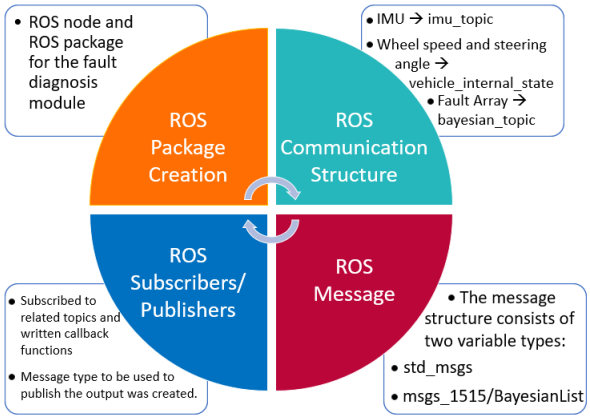

Figure 3. ROS structure of the fault diagnosis algorithm.

2.7. ROS Structure

Human-Machine Interface (HMI) can be defined as software or hardware that provides the basic interaction between humans and vehicles via communicating through communication methods and protocols such as CAN and ROS. Modern HMIs are designed to provide intuitive control, display systems and include a variety of functions such as entertainment, navigation and autonomous driving assistance systems. Additionally, the user can observe some basic sensor outputs through the HMI.

The HMI that has been developed consists of 4 main pages, grouped according to frequency of use and interrelatedness. The first page contains the main HMI page, which includes lane and road information, environmental obstacles, TSLR (Traffic Light and Sign Recognition) information, decision maker decisions and possibilities, a small navigation map, and ACC (Adaptive Cruise Control) controls (Figure 4). The second page is the indicator page that shows the desired and actual speed and the actual and desired steering angles. The third page is the main map and navigation page (Figure 5) and finally there is the diagnostics page. The project has been developed using ReactJS technology. All data communication between the HMI and the vehicle is provided via ROS.

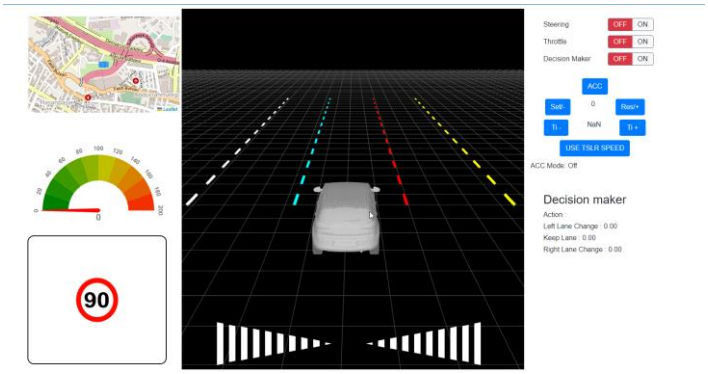

Figure 4. HMI Main Page.

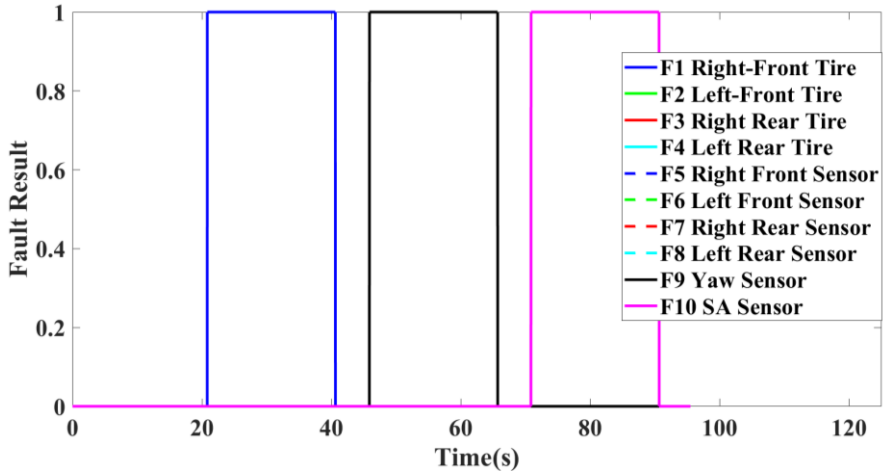

Figure 5. Fault Result.

3. Test Scenarios

Tests of the fault detection algorithm integrated into ROS have been carried out using real vehicle data. During the test, values were added to the data collected on the real vehicle in a way that would cause a fault in the desired sensor at that moment. The test scenarios selected here are the right and left front wheel speed sensors, respectively. Here, one of the main reasons why faulty reading have been injected to the speed sensors is to demonstrate that the Bayesian Network can detect this situation when there is a fault in the speed sensors, and then the speed value obtained from the EKF starts to be used instead of the speed value from the wheel speed sensor in the dynamic bicycle model.

In order to perform fault detection, the threshold value of each residual has been determined. Real vehicle test data has been again used to determine this threshold value. By examining ten fault free datasets of the test vehicle, threshold values have been set for each residual value and these values are shown in Table 4. In cases where the calculated residual values exceed these threshold values, that residual value will be assigned as 1, and in cases where it does not exceed these thresholds, it will be assigned as 0.

Table 4. Residual thresholds for each residual.

Residual	Threshold Value
R_1, R_2, R_3	0.2 rad/s
R_4, R_5	0.02
R_6	0.4 rad

3.1. Test Scenarios

After integrating the fault diagnosis algorithm into the vehicle, we conducted tests in a controlled traffic-free area. While performing tests within the vehicle, we manipulated the incoming data to create fault scenarios and observe whether the algorithm functioned correctly. To test the algorithm, three fault scenarios are created. First, values for residuals R_1, R_2 and R_4 are triggered, and it resulted in a fault on F_1 which corresponds to the front tire. Then, the values for residuals R_1-R_2-R_3 and R_6 are triggered, and it indicated a fault in F_9 which corresponds to yaw rate sensor. Finally, when values for residuals R_1 and R_6 are triggered, a fault in F_{10} which corresponds to the steering angle was observed. The fault results are shown in Figure 6 below. The time points at which each residual is triggered can be seen in Figures 7–9.

Furthermore, in the algorithm design, we implemented an additional function to prevent the system from faulting due to anomaly jumps in residual values, ensuring that the system would not go into fault mode before reaching a certain number of cycles.

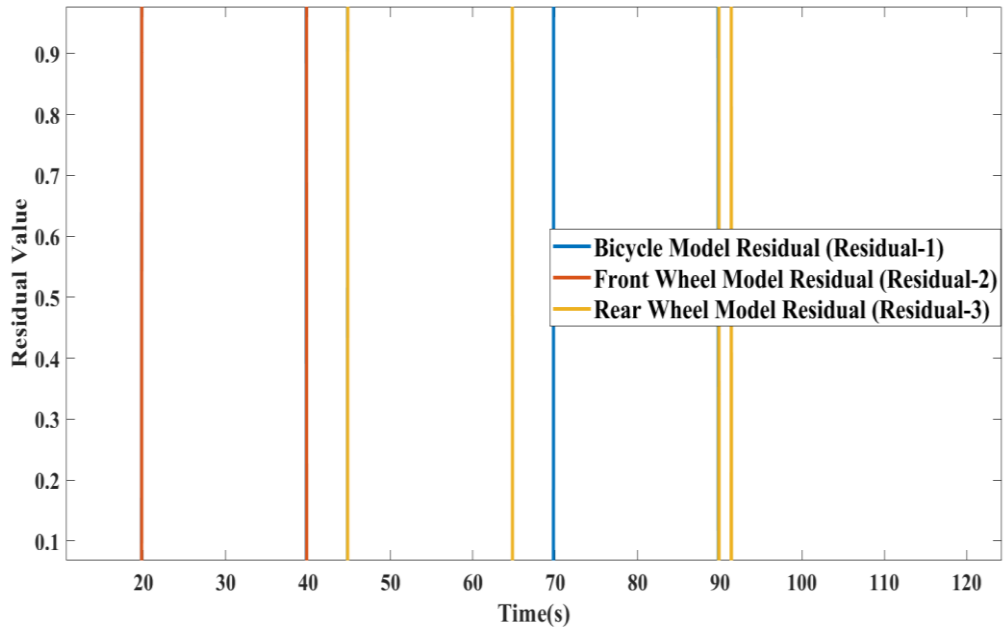

Figure 6. R_1-R_2-R_3 Residuals.

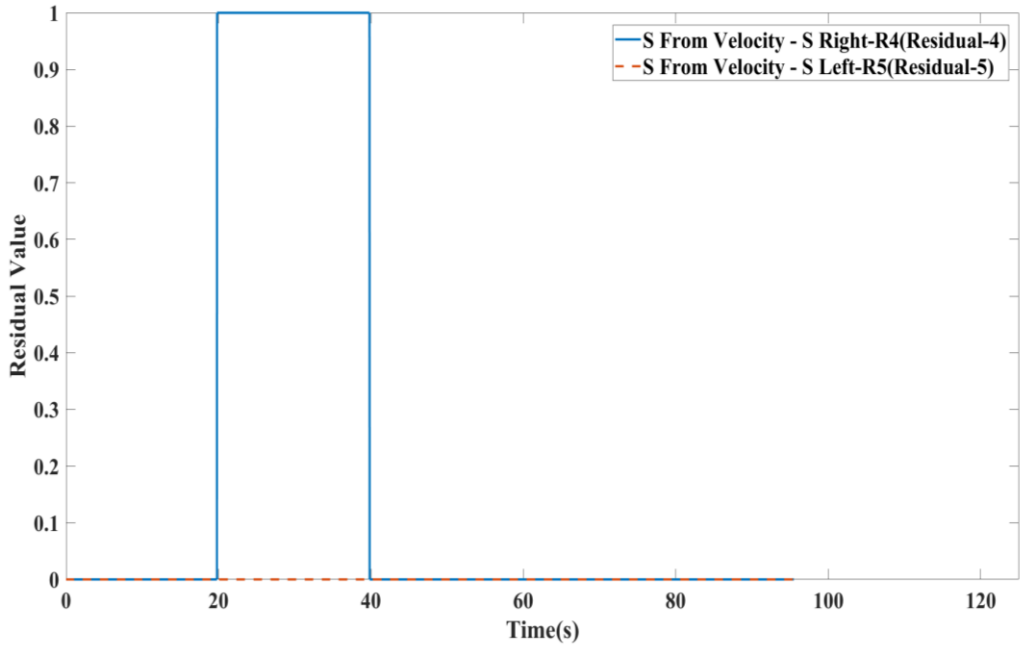

Figure 7. R_4–R_5 Residuals.

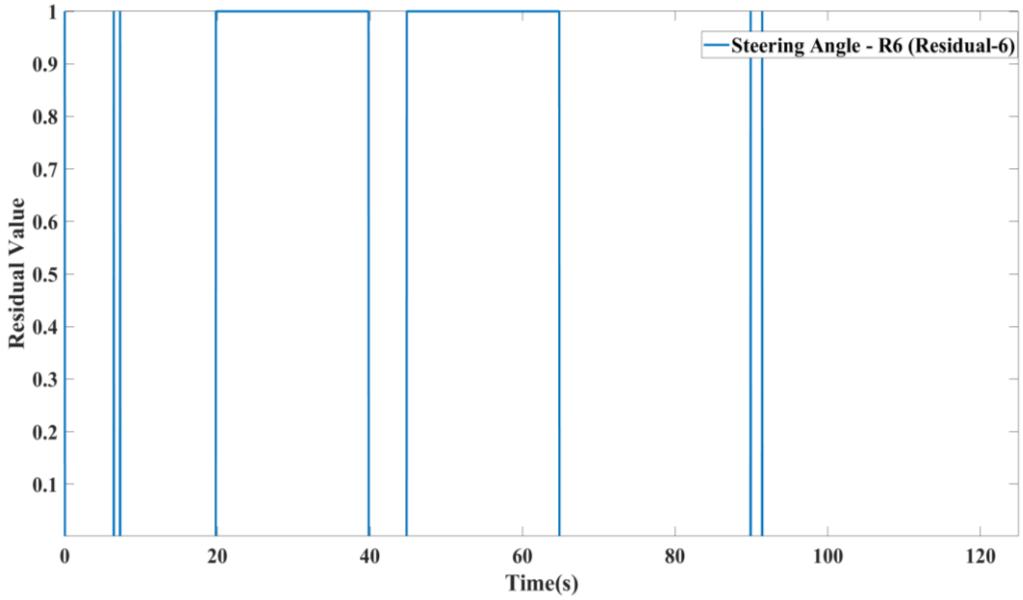

Figure 8. R_6 Residual.

The faults have been determined based on Table 3. Additionally, these residuals and faults are also visible on the HMI as given in Figures 10–12, depending on the residual values.

Figure 9. Right Front Tire Fault on HMI Screen.

Figure 10. Yaw Rate Fault on HMI Screen.

Figure 11. Steering Angle Fault on HMI Screen.

4. Results

In this study, a model-based fault detection method with dynamically adjusted conditional probability distributions is described. This proposed method uses both a Bayesian network structure and EKF. At this point, the vehicle's speed data is obtained by combining the data obtained from the GPS sensor and IMU sensor with the help of EKF. If there is a faulty measurement from any wheel sensor, the speed data obtained with the help of EKF will be used instead of the wheel speed data, preventing the incorrect calculation of the yaw rate value via the bicycle model. The yaw rate measured by the gyroscope sensor has been compared with the yaw rates calculated by three analytical models (front wheel, rear wheel, and bicycle dynamic model). Apart from the yaw rate, the slip rate obtained using the measurements of the left and right wheels has been compared to the slip rates calculated by the wheel model for both the front and rear wheels. In addition, the value obtained from the steering angle sensor was compared with the steering angle calculated from the model. As a result of comparing these sensor and model values, six residual values have been obtained. Following the integration of the fault diagnosis algorithm into the vehicle, we conducted trials in a controlled, traffic-free environment. During these vehicle-based tests, we deliberately manipulated incoming data to simulate fault scenarios and monitored the algorithm's performance to ensure it operated correctly. As a result, in

real-time tests, the algorithm that use both the Bayesian network and EKF successfully detected faults related to the lateral dynamics of the vehicle and the results have been successfully displayed on the HMI.

Author Contributions: Conceptualization, T.B., M.M.G., B.K. and E.A.; methodology, T.B., M.M.G. and B.K.; software, T.B., M.M.G., B.K. and E.A.; validation, T.B., M.M.G. and B.K.; investigation, T.B., M.M.G. and B.K.; supervision, T.B. All authors have read and agreed to the published version of the manuscript.

Funding: This research received no external funding.

Institutional Review Board Statement: Not applicable.

Informed Consent Statement: Not applicable.

Data Availability Statement: Data sharing Does not apply to this paper.

Conflicts of Interest: The authors declare no conflict of interest.

References

1. Ko, C.; Fox, D. GP-BayesFilters: Bayesian filtering using Gaussian process prediction and observation models. *Int. J. Robot. Res.* **2009**, *28*, 1524–1547.
2. Zhong, M.; Xue, T.; Ding, X. A survey on model-based fault diagnosis for linear discrete time-varying systems. *Neurocomputing* **2018**, *306*, 51–60.
3. Chen, J.; Patton, R.J. *Robust Model-Based Fault Diagnosis for Dynamic Systems*; Kluwer Academic Publishers: Dordrecht, The Netherlands, 1999.
4. Raghuraman, S.; Mahadevan, S. Fault detection and diagnosis using dynamic Bayesian networks and system identification. *J. ProcessControl.* **2010**, *20*, 604–616.
5. Ding, S.X. *Model-Based Fault Diagnosis Techniques: Design Schemes, Algorithms, and Tools*; Springer: Berlin, Germany, 2008.
6. Marzat, J.; Lahanier, H.P.; Damongeot, F.; Walter, E. Model-based fault diagnosis for aerospace systems: A survey. *Proc. Inst. Mech. Eng. Part G J. Aerosp. Eng.* **2011**, *226*, 1329–1360.
7. Ji, L.; Zhang, Y.; Yan, R.; Song, Y. Fault diagnosis of power transformers based on fault tree and fault tree-analytic hierarchy process. *Electr. Power Syst.Res.* **2019**, *174*, 105822.
8. Huang, Y., McMurran, R., Dhadyalla, G. et al. Probability based vehicle fault diagnosis: Bayesian network method. *J. Intell. Manuf.* **2008**, *19*, 301–311.
9. Huang, B.; Zhu, Q.; Zhang, D.; Li, X. A survey of signal processing techniques for rotating machinery fault diagnosis. *Measurement* **2019**, *136*, 597–619.
10. Harihara, P.P.; Kim, K.; Parlos, A.G. Signal-based versus model-based fault diagnosis-a trade-off in complexity and performance. In Proceedings of the 4th IEEE International Symposium on Diagnostics for Electric Machines, Power Electronics and Drives, 2003. SDEMPED 2003, Atlanta, GA,USA, 24–26 August 2003; pp. 277–282.
11. Bodrumlu, T.; Gözüm, M.M.; Kavak, B. Enhanced Fault Detection of Vehicle Lateral Dynamics Using a Dynamically Adjustable Bayesian Network Structure and Extented Kalman Filter. In Proceedings of the ASME 2022 International Mechanical Engineering Congress and Exposition, Columbus, Ohio, USA, 30 October–3 November 2022; ASME: New York, NY, USA, 2022; Volume 9, No. V009T14A024.
12. Cibooğlu, M. Hybrid Controller Approach for an Autonomous Ground Vehicle Path Tracking Problem. M.Sc. Thesis, Dept. Cont. Autom. Eng., Istanbul Technical University, Istanbul, Turkey, 2016.
13. Fischer, D.; Börner, M.; Schmitt, J.; Isermann, R. Fault detection for lateral and vertical vehicle dynamics. *Control Eng. Pract.* **2007**, *15*, 315–324.
14. Schwall, M.L.; Gerdes, J.C. Multi-modal Diagnostics for Vehicle Fault Detection. In Proceedings of the ASME 2001 International Mechanical Engineering Congress and Exposition, New York, NY, USA, 11–16 November 2001; ASME International Mechanical Engineering Congress and Exposition: New York, NY, USA, 2001.
15. Miller, S.L.; Youngberg, B.; Millie, A.; Schweizer, P.; Gerdes, J.C. Calculating Longitudinal Wheel Slip and Tire Parameters Using GPS Velocity. In Proceedings of the American Controls Conference, Arlington, VA, USA, 25–27 June 2001; pp. 1800–1805.

Disclaimer/Publisher's Note: The statements, opinions and data contained in all publications are solely those of the individual author(s) and contributor(s) and not of MDPI and/or the editor(s). MDPI and/or the editor(s) disclaim responsibility for any injury to people or property resulting from any ideas, methods, instructions or products referred to in the content.